1.55 m. The overstory was dominated by loblolly pine (*Pinus taeda*) across stand types. In high mortality stands, fine and coarse woody debris such as bark and needles from dead loblolly pines cover the soil surface.

2.2. Soil and rainwater collection

Soils from pre-hurricane loblolly forest and baldcypress forest were collected in Spring of 2022 within two weeks to minimize differences in abiotic conditions between sampling dates. Hurricane Ian made landfall

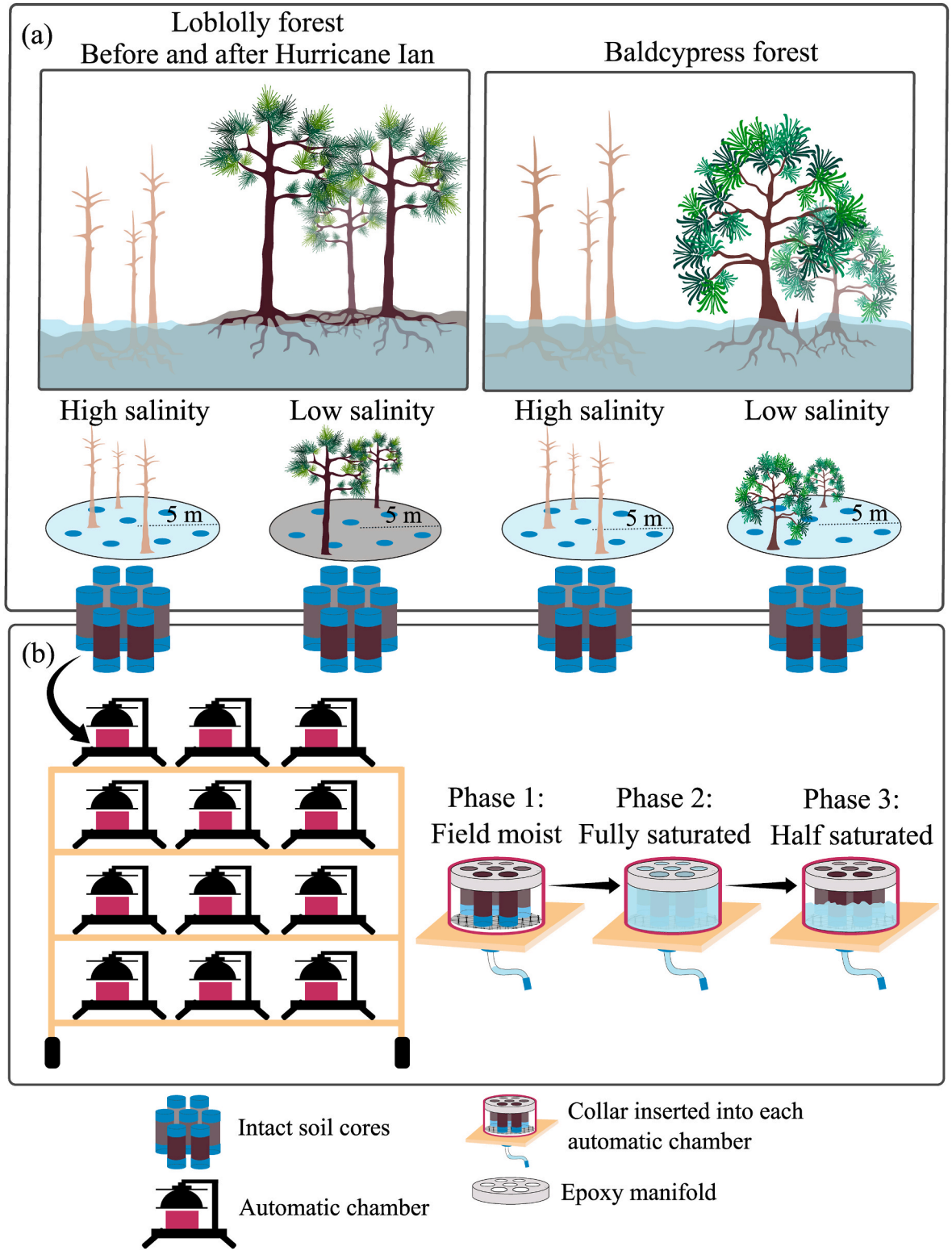

Fig. 1. Schematic diagram of sampling and mesocosm design which includes (a) *in situ*, intact soil core collection from high and low salinity stands in a freshwater wetland dominated by baldcypress and an upland forest dominated by loblolly and (b) a novel mesocosm design for measuring greenhouse gas fluxes from replicates of intact cores with controlled flooding.

on September 30, 2022 near Georgetown, SC as a category 1 hurricane with a peak wind gust of 37 m s^{-1} measured near the site (Armstrong, 2022). Initial landfall was slightly south of the research site such that onshore winds, coinciding with local high tide, generated a storm surge of approximately 1.8 m. Immediately after landfall, the storm turned north such that the eye passed over the research plots. On October 10th, 2022, we resampled at the loblolly forest study site in response to the hurricane Ian storm surge, which pulsed seawater into high and low salinity stands. Samples collected before pulsed salinity from Hurricane Ian are hereafter referred to as "pre-hurricane loblolly" and samples collected after pulsed salinity from Hurricane Ian will hereafter be referred to as "post-hurricane loblolly". Within baldcypress and loblolly forests, we sampled from six high and six low salinity stands (Fig. 1a). We used a 5.08 cm diameter corer to collect 7 intact soils cores from 0 to 10 cm depth beneath the litter layer. Sample locations were chosen randomly to capture heterogeneity at the plot scale. Intact soil cores were capped on both ends. All cores were bagged, placed on ice in an upright position and transported back to lab where our water addition experiment took place. Prior to sampling, we drilled holes in the lower caps and lined them with fine mesh. These caps were used on the bottom of the intact cores to allow water movement through the core while preventing soil loss.

Prior to each experiment, we used thoroughly rinsed metal troughs to collect freshly fallen rainwater in large glass containers, which was later added to soil cores in our lab mesocosm. We ensured that the rainwater did not contact anything other than the metal trough before entering the glass containers, thereby minimizing contamination.

2.3. Greenhouse gas measurement

Soil greenhouse gas fluxes were measured with multiplexed, automated soil flux chambers attached to mesocosms and coupled with an online mass spectrometer for high frequency, real-time gas flux measurements. Systems with identical major components have been described in lab mesocosm experiments (Petrakis et al., 2017) and field deployments (Courtois et al., 2019; Petrakis et al., 2018). The unique configuration of our system is described in the supplemental methods (Section S1).

Mesocosms (Fig. 1b) were constructed by sealing 20 cm diameter PVC pipe to a flat PVC base to create a watertight reservoir, with a drain valve at the bottom. An epoxy manifold was created to hold and create an airtight seal around seven 5.08 cm diameter soil cores in their plastic sampling sleeves, and the wall of the reservoir. The seven soil cores within a single mesocosm rest on a layer of plastic mesh that provides hydraulic connectivity between the cores, allowing them to be flooded and drained to the same level. Top caps were removed before placing the cores into the chambers and beginning gas measurements. Each measurement lasted 4 min and 45 s with a 60 s prepurge, 180 s observation and 45 s post-purge such that CH_4 and CO_2 concentrations were measured in each chamber approximately once an hour over the length of our six day experiment. The specifics of our flux calculations are described in the supplementary methods (Section S1).

We applied two quality control procedures to all calculated fluxes before proceeding with analysis. First, samples with a CO_2 or CH_4 flux below the minimum detectable flux (MDF) of the Picarro analyzer were assigned a gas flux equal to the MDF. We followed the methods of Courtois et al. (2019) to calculate MDF using the following equation in which A_a is the analytical accuracy of the Picarro G2508 (10 ppb for CH_4 and 600 ppm for CO_2), t_c is the time the chamber lid was closed for measurement in seconds, n is the number of gas concentration measurements used to calculate the flux (assuming one measurement per second), V is the chamber volume (0.0040761 m^3), P is atmospheric pressure (101325 Pa), S is the surface area of exposed soil within the chamber (0.01477 m^2), R is the ideal gas constant (8.314 m^3 Pa K^{-1} mol^{-1}) and T is the ambient temperature (298.15 K):

$$MDF = \left(\frac{A_a}{t_c\sqrt{n}}\right)\left(\frac{VP}{SRT}\right) \quad \text{Eqn.2}$$

There were no samples with CO_2 fluxes below the CO_2 MDF of 3.20 mmol m^{-2} s^{-1}, but 752 of 10,443 total CH_4 fluxes were below the CH_4 MDF and were therefore assigned a value of the CH_4 MDF, 0.05 mmol m^{-2} s^{-1}. For the second step in our quality control procedure, similar to Petrakis et al. (2018), we filtered out all fluxes that did not meet at least one of the following criteria: 1) $R^2 > 0.90$ or 0.80 for CO_2 and CH_4, respectively, and/or 2) flux is close to zero. To define fluxes that were close to zero, we used the standard deviation of the absolute value of all CO_2 and CH_4 fluxes with $R^2 < 0.90$ or 0.80, respectively; fluxes less than one standard deviation were considered close to zero and therefore remained in the dataset regardless of their R^2 value, while fluxes greater than one standard deviation that did not meet the R^2 requirements were removed from the dataset. At this quality control step, we removed 38 CO_2 fluxes and 76 CH_4 fluxes.

To understand the effects of freshwater inundation and the potential for antecedent salinity to mediate the effects of freshwater inundation on soil GHG emissions, we carried out three phases of water addition (Fig. 1b). In the first phase, which lasted 24 h, no rainwater was added to the collars, but water was able to slowly drain from the bottom of the cores, potentially increasing oxygen availability in soil cores that were saturated in the field, but not altering the redox state of cores that were unsaturated in the field. In the second phase, which lasted 48 h, we filled soil collars with rainwater to fully saturate all soil cores. Throughout this phase, we poured rainwater into the top of the soil cores twice a day to ensure that the soils remained fully saturated. Finally, in the third phase, which lasted 72 h, we fully drained each collar and then returned 1.25 L of this water back into the collar so that soil cores were approximately half saturated.

2.4. Soil chemical analyses

To understand the effects of chronic salinization and associated tree mortality on soil chemical properties we combined the seven intact cores from each replicate plot into one composite soil sample after the laboratory experiment ended. We analyzed all composite samples for soil moisture, pH and conductivity and for composite samples from baldcypress and pre-hurricane loblolly forests, we analyzed soil organic matter (SOM) content and C and N concentrations (Table 1). We quantified soil electrical conductivity, a measurement of soil salinity in this study, and pH in a 2:1 (deionized water: soil; by dried mass) slurry. We oven-dried a root-free subsample of each composite soil sample at 105 °C for 24 h to determine gravimetric soil moisture, and ashed a separate root-free subsample in a muffle furnace at 550 °C for 3 h to determine organic matter content. The remaining soil was air dried, ground and analyzed for total C and N using an elemental analyzer (Flash-2000, Thermo Scientific, Waltham, Massachusetts, USA). We calculated C and N concentrations by multiplying percent C or N by total sample dry mass and then dividing by total sample volume.

2.5. Statistical analyses

Statistical analyses were carried out in R 1.2.5033 (R Development Core Team, 2019). Statistical significance was determined based on $P < 0.05$. Prior to statistical analyses, continuous gas concentration measurements were processed into hourly intervals by averaging CO_2 and CH_4 fluxes across the six chambers from high salinity stands and six chambers from low salinity stands resulting in one flux measurement for each forest type each hour of our experiment.

To test for the effect of chronic saltwater inundation on soil chemical properties and greenhouse gas fluxes, we conducted two-way ANOVAs with forest type (loblolly, baldcypress), stand type (high salinity, low salinity) and the interaction between forest type and stand type as fixed

Table 1
Soil chemical properties for high and low salinity stands within a freshwater swamp dominated by cypress and an upland forest dominated by loblolly before and after pulsed salinity from Hurricane Ian (mean ± SD, n = 6).

Forest type	Salinity	Soil chemical property								
		Soil moisture (g H_2O g dry soil^{-1})	pH	Conductivity (ms cm^{-1})	SOM content (g OM g dry soil^{-1})	Bulk density (g dry soil cm^{-3})	C concentration (g C cm^{-3})	C concentration (mol C cm^{-3})	N concentration (g N cm^{-3})	C:N mass ratio
Baldcypress	High	$8.88 \times 10^{-1} \pm 1.31 \times 10^{-2}$	$4.77 \pm 2.36 \times 10^{-1}$	10.78 ± 1.94	$7.03 \times 10^{-1} \pm 6.41 \times 10^{-2}$	$2.84 \times 10^{-2} \pm 1.82 \times 10^{-3}$	$1.09 \times 10^{-2} \pm 4.79 \times 10^{-4}$	$9.05 \times 10^{-1} \pm 3.99 \times 10^{-2}$	$5.61 \times 10^{-4} \pm 4.10 \times 10^{-5}$	19.49 ± 1.83
Baldcypress	Low	$7.56 \times 10^{-1} \pm 3.90 \times 10^{-2}$	$4.97 \pm 1.11 \times 10^{-1}$	4.52 ± 2.49	$3.73 \times 10^{-1} \pm 4.61 \times 10^{-2}$	$5.29 \times 10^{-2} \pm 1.44 \times 10^{-2}$	$9.19 \times 10^{-3} \pm 2.13 \times 10^{-3}$	$7.66 \times 10^{-1} \pm 1.77 \times 10^{-1}$	$5.48 \times 10^{-4} \pm 1.36 \times 10^{-4}$	$16.90 \pm 8.13 \times 10^{-1}$
Loblolly (pre-hurricane)	High	$6.77 \times 10^{-1} \pm 4.81 \times 10^{-2}$	$4.51 \pm 1.42 \times 10^{-1}$	$1.03 \pm 1.60 \times 10^{-1}$	$2.12 \times 10^{-1} \pm 4.10 \times 10^{-2}$	$1.12 \times 10^{-1} \pm 1.61 \times 10^{-2}$	$1.15 \times 10^{-2} \pm 1.54 \times 10^{-3}$	$9.57 \times 10^{-1} \pm 1.28 \times 10^{-1}$	$4.12 \times 10^{-4} \pm 6.20 \times 10^{-5}$	27.97 ± 1.12
Loblolly (pre-hurricane)	Low	$3.93 \times 10^{-1} \pm 6.06 \times 10^{-2}$	$3.70 \pm 2.18 \times 10^{-1}$	$1.54 \times 10^{-1} \pm 3.60 \times 10^{-2}$	$1.23 \times 10^{-1} \pm 3.43 \times 10^{-2}$	$1.48 \times 10^{-1} \pm 2.75 \times 10^{-2}$	$8.26 \times 10^{-3} \pm 9.39 \times 10^{-4}$	$6.88 \times 10^{-1} \pm 7.81 \times 10^{-2}$	$2.80 \times 10^{-4} \pm 1.50 \times 10^{-5}$	29.47 ± 2.47
Loblolly (post-hurricane)	High	$5.93 \times 10^{-1} \pm 2.47 \times 10^{-2}$	$4.25 \pm 2.02 \times 10^{-1}$	6.72 ± 1.21	$1.85 \times 10^{-1} \pm 1.21 \times 10^{-2}$					
Loblolly (post-hurricane)	Low	$6.11 \times 10^{-2} \pm 1.97 \times 10^{-2}$	$3.63 \pm 1.00 \times 10^{-1}$	$2.51 \pm 6.31 \times 10^{-1}$	$2.15 \times 10^{-1} \pm 1.05 \times 10^{-2}$					

**Soil pH and electrical conductivity were measured in a 2:1 (deionized water: soil; by dried mass) slurry.

effects. To test for the direct effects of pulsed salinity as well as the potential for chronic salinization to mediate the effects of pulsed salinity on soil chemical properties and greenhouse emissions, we conducted two-way ANOVAs with sample date (pre-hurricane, post-hurricane), stand type and the interaction between sample date and stand type as fixed effects. We performed pairwise comparisons between each level of forest type, stand type and sample date using the "emmeans" function in the emmeans package (Russell, 2021), with Tukey's adjustment method for multiple comparisons. To test for the effect of inundation on greenhouse gas fluxes and soil chemical properties within each combination of forest type and stand level mortality, we conducted one-way ANOVAs with water inundation phase as a fixed effect. We performed post-hoc pairwise comparisons between water inundation phases using Tukey honestly significant difference (HSD) tests. For all models, CH_4 fluxes, CO_2 fluxes, pH, electrical conductivity, SOM content, C concentration, N concentration and C:N ratios served as dependent variables. However, soil C and N concentrations and C:N ratios were not measured in post-hurricane loblolly soils. To test for correlations between

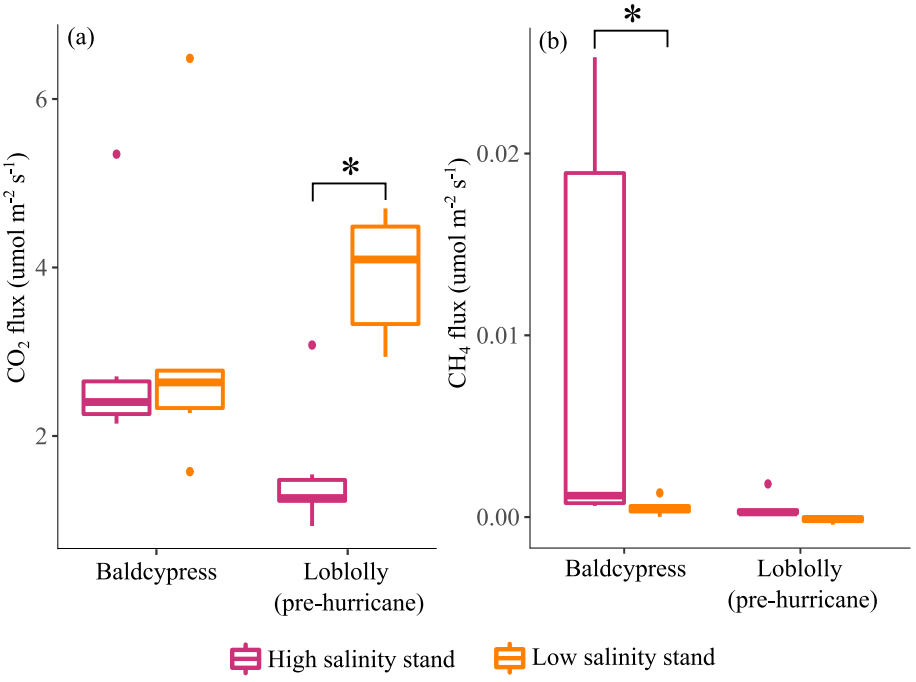

Fig. 2. Boxplot illustrating the effects of chronic saltwater exposure and associated tree mortality and tree mortality on (a) soil carbon dioxide (CO_2) fluxes and (b) soil methane (CH_4) fluxes across a freshwater swamp dominated by baldcypress and an upland forest dominated by loblolly. Data from high salinity stands and low salinity stands are represented by pink and orange, respectively. Carbon dioxide fluxes were significantly greater in low compared to high salinity stands in loblolly forest ($p < 0.001$), but there was no effect of stand mortality on CO_2 fluxes in baldcypress forest ($p = 0.93$). In contrast, CH_4 fluxes were significantly greater in high compared to low salinity stands in baldcypress forest ($p = 0.01$), but this effect was not significant in loblolly forest ($p = 0.21$). Asterisks denote significant differences between stand types.

greenhouse gas fluxes and soil chemical properties, we constructed linear models with CO_2 and CH_4 fluxes as the dependent variables and pH, conductivity, C concentration, N concentration, C:N ratios and SOM content as the independent variables. Finally, to assess variability in soil chemical properties (C concentration, N concentration, C:N ratios, SOM content, pH and conductivity) among samples in multivariate space, we performed a principal components analysis (PCA) with centered and scaled data using the "prcomp" function in the stats package (R Development Core Team, 2019).

3. Results

3.1. Effects of chronic and pulsed salinity on GHG fluxes

The effect of chronic salinization and associated tree mortality on CO_2 fluxes depended on forest type with significantly greater CO_2 fluxes in high compared to low salinity stands in loblolly forest ($p < 0.001$), but no effect of stand level mortality on CO_2 fluxes in baldcypress forest (Fig. 2a). Furthermore, we found no effect of a hurricane related storm surge on CO_2 fluxes in a loblolly forest ($F_{1,20} = 0.44$, $p = 0.51$), with greater CO_2 fluxes in high compared to low salinity stands before and after the pulsed salinity ($p < 0.001$ for pre- and post-hurricane forest). Across baldcypress and loblolly forest, greater CO_2 fluxes correlated significantly with lower soil C (baldcypress, $R^2 = 0.59$, $p = 0.002$; loblolly, $R^2 = 0.21$, $p = 0.07$) and N (baldcypress, $R^2 = 0.51$, $p = 0.005$; loblolly, $R^2 = 0.29$, $p = 0.04$) concentrations. SOM content exhibited a significant negative relationship with CO_2 fluxes in loblolly forest ($R^2 = 0.26$, $p = 0.05$), but there was no significant correlation between these variables in baldcypress forest.

Across soils sampled before and after a hurricane related storm surge, we found a significant positive correlation between conductivity and CH_4 fluxes ($R^2 = 0.39$, $p = 0.001$; Fig. 3b) driven by two distinct relationships. First, CH_4 fluxes were greater from higher relative to lower salinity stands ($F_{1,20} = 30.78$, $p < 0.001$) across pre- ($p < 0.001$) and post- ($p < 0.001$) hurricane sample dates (Fig. 3a). Second, CH_4 fluxes from higher conductivity post-hurricane loblolly forest were greater than CH_4 fluxes from lower conductivity pre-hurricane loblolly forest ($F_{1,20} = 9.08$, $p = 0.007$) across high and low salinity stands ($p = 0.04$, 0.05, respectively). In pre-hurricane loblolly forest, no soil chemical properties we measured other than conductivity correlated significantly with CH_4 fluxes, but in post-hurricane loblolly forest, pH correlated positively ($R^2 = 0.72$, $p < 0.001$) and SOM content correlated negatively ($R^2 = 0.40$, $p = 0.02$) with CH_4 fluxes.

We found significantly greater CH_4 fluxes from higher conductivity and mortality forest stands relative to lower conductivity and mortality stands in baldcypress forest ($F_{1,20} = 7.78$, $p = 0.01$; Fig. 2b). In baldcypress forest, soil C:N ratios exhibited a significant positive relationship with CH_4 fluxes (C:N, $R^2 = 0.70$, $p < 0.001$; pH, $R^2 = 0.44$, $p = 0.01$). No other soil chemical properties we measured correlated significantly with CH_4 fluxes in baldcypress forest.

3.2. Effects of forest type and chronic salinization on soil chemical properties

Most measured soil chemical properties differed significantly between loblolly and baldcypress forest types and between high and low salinity stands except for SOM content which was similar across all treatments and soil C:N ratios which did not differ between high and low salinity stands (Table 1). Soil pH, conductivity and N concentrations were significantly greater in baldcypress compared to loblolly forest across stand types (pH, $F_{1,\ 20} = 103.64$, $p < 0.001$; conductivity, $F_{1,20} = 348.06$, $p < 0.001$; N concentration, $F_{1,20} = 42.34$, $p < 0.001$) and in high compared to low salinity stands across forest types (pH, $F_{1,20} = 16.44$, $p < 0.001$; conductivity, $F_{1,20} = 95.11$, $p < 0.001$; N concentration $F_{1,20} = 8.82$, $p = 0.088$). Similar to N concentrations, C concentrations were significantly greater in high compared to low salinity stands across forest types ($F_{1,20} = 18.01$, $p < 0.001$), but opposite to N concentrations, C concentrations did not differ between baldcypress and loblolly forest types. Soil C:N ratios were significantly greater in loblolly compared to baldcypress forest across stand types ($F_{1,20} = 233.75$, $p < 0.001$), but the effect of stand type on C:N ratios were only significant in baldcypress forest where C:N ratios were greater in low compared to high salinity stands.

In a PCA defined by soil all measured soil chemical properties, high and low salinity stands in baldcypress forest grouped separately from high salinity stands in loblolly forest which grouped separately from low salinity stands in loblolly forest (Fig. 4). The three groups separated most clearly along PC1 which explained 56.06% of total variability between samples. The largest contributions to variance explained by PC1 came from N concentration (26.76%), pH (23.78%), C:N ratios (23.31%) and conductivity (18.67%). Carbon concentration (49.1%) and SOM content (37.43%) contributed most to PC2 which explained

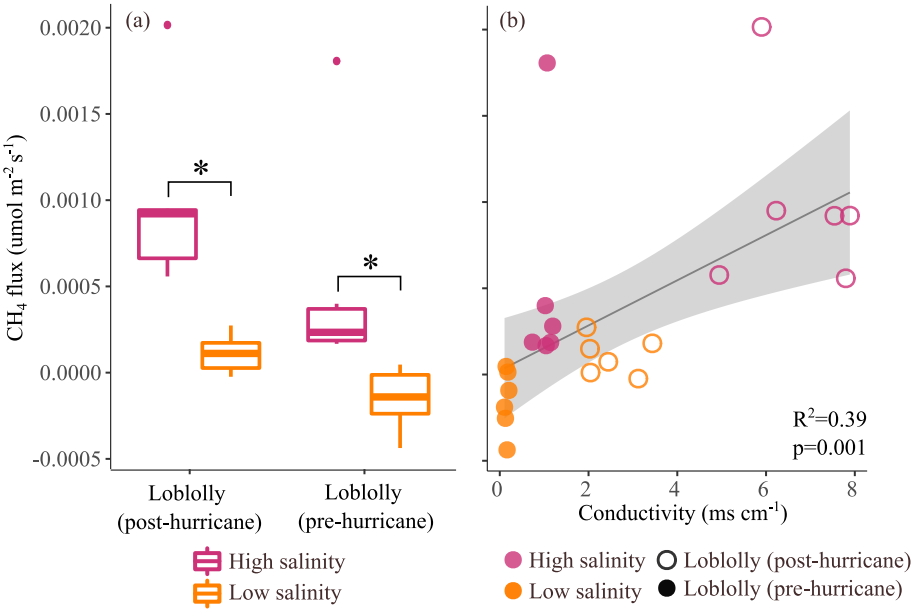

Fig. 3. Effects of chronic and pulsed salinity on CH_4 fluxes in a loblolly forest illustrated using (a) a boxplot comparing CH_4 fluxes in high versus low salinity stands before and after a hurricane related storm surge and (b) a regression between CH_4 fluxes and soil salinity across pre- and post-hurricane sample dates. Data from high and low salinity stands are represented by pink and orange, respectively while data from pre- and post-hurricane sample dates are represented by open and closed circles, respectively. Methane fluxes were significantly greater in higher salinity high salinity stands relative to lower salinity low salinity stands ($F_{1,20} = 30.78$, $p < 0.001$) across pre- and post-hurricane sample dates ($p = 0.001$, $p < 0.001$, respectively). There is a significant positive relationship between salinity and CH_4 fluxes from *in situ*, intact soil cores collected in loblolly forest before and after a hurricane related storm surge ($R^2 = 0.39$, $p = 0.001$). Asterisks denote significant differences between stand types.

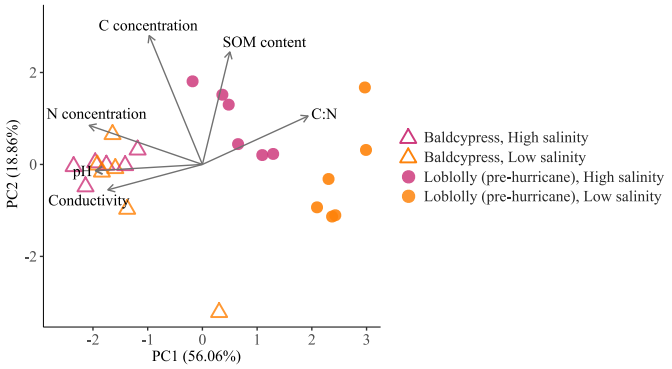

Fig. 4. Principal component analysis (PCA) plot defined by the following soil chemical properties: carbon concentration, nitrogen concentration, C:N ratios, soil organic matter content, pH and conductivity. Baldcypress and pre-hurricane loblolly forest types are denoted by open triangles and closed circles, respectively, while high and low salinity stand types are denoted by pink and orange, respectively. The largest contributions to variance described by PC1 are N concentration (26.76%), pH (23.78%), C:N ratio (23.31%) and conductivity (18.67%) while the largest contributions to variance described by PC2 are C concentration (49.10%) and SOM content (37.43%).

18.89% of the total variance.

3.3. Effect of inundation on CO_2 and CH_4 fluxes

We found a significant effect of water addition phase on soil CO_2 fluxes across high and low salinity stands (loblolly pre-hurricane, high, $F_{2,15} = 10.56$, $p = 0.001$; loblolly pre-hurricane, low, $F_{2,15} = 34.51$, $p < 0.001$; baldcypress, high, $F_{2,15} = 45.8$, $p < 0.001$, baldcypress, low, $F_{2,15} = 20.12$, $p < 0.001$), but the effect of water addition phase on CH_4 fluxes was only significant in low salinity stands (loblolly pre-hurricane, low, $F_{2,15} = 27.59$, $p < 0.001$; baldcypress, low, $F_{2,15} = 9.77$, $p = 0.002$; Fig. 5a–d). Soil CO_2 fluxes from fully saturated soil cores were significantly lower than CO_2 fluxes from field moist soil cores (loblolly pre-hurricane, high, $p = 0.001$; loblolly pre-hurricane, low, $p < 0.001$; baldcypress, high, $p < 0.001$; baldcypress, low, $p < 0.001$) or half saturated soil cores (loblolly pre-hurricane, high, $p = 0.02$; loblolly pre-hurricane, low, $p = 0.002$; baldcypress, high, $p < 0.001$; baldcypress, low, $p < 0.001$) (Fig. 5ab). However, we found similar CH_4 fluxes from field moist and fully saturated soil cores across high and low salinity stands of baldcypress forest, and in high salinity stands of loblolly forest. In contrast, CH_4 fluxes were greater in fully saturated relative to field moist soil cores in low salinity stands of loblolly forest ($p < 0.01$; Fig. 5cd).

Differences in CO_2 and CH_4 fluxes between field moist and half saturated water addition phases varied among treatments. Specifically, CO_2 fluxes were greater in half saturated relative to field moist soils in low salinity stands of loblolly forest ($p = 0.003$) but did not differ between phases in low salinity stands of loblolly forest or in high or low salinity stands of baldcypress forest (Fig. 5ab). Furthermore, CH_4 fluxes were greater in half saturated relative to field moist soils in low salinity stands of loblolly ($p < 0.001$) and baldcypress forest ($p = 0.006$), but this effect was not significant in high salinity stands (Fig. 5cd).

4. Discussion

Salinization and freshwater inundation of coastal forest soils caused by sea level rise and intensifying storms can have direct and indirect effects on soil carbon cycling (Chen et al., 2023; Norwood et al., 2021; Servais et al., 2019; Stagg et al., 2017), yet the potential for these novel conditions to feed back with climate change through altered greenhouse gas emissions is not well understood. In this study, we aimed to address this gap in knowledge through the following hypotheses: 1) chronic salinization and associated tree mortality will decrease soil CO_2 production by altering the quantity and quality of soil organic matter, 2) underlying exposure to chronic salinization at the stand scale will mediate the effects of pulsed salinity from a storm surge on CH_4 fluxes and 3) freshwater inundation will cause a shift from aerobic to anaerobic respiration particularly in lower salinity stands. Overall, we demonstrated the potential for differences in soil conditions and associated tree mortality across forest types to mediate the effects of sea level rise and storm surges on greenhouse gas fluxes from coastal systems.

4.1. Effect of chronic salinization and associated tree mortality on CO_2 fluxes

The effect of chronic salinization and associated tree mortality on CO_2 fluxes across forest types may be mediated by environmental context, driving distinct patterns in a freshwater baldcypress swamp relative to an upland loblolly forest. Specifically, differences in soil chemical properties between stand types correlated with a significant effect of chronic salinization and tree mortality on CO_2 fluxes in loblolly forest while similar soil chemical properties across stand types correlated with no effect of chronic salinization and associated tree mortality on CO_2 fluxes in baldcypress forest. Although decreased productivity and tree death due to chronic salinization can decrease the supply of labile C to limit microbial respiration (King et al., 2002; Megonigal et al., 1999), we found a negative relationship between soil C concentrations and CO_2 fluxes and no significant relationship between soil C:N ratios or SOM content and CO_2 fluxes in loblolly forest. Therefore, differences in CO_2 production between stand types may not be controlled by SOM quantity or quality in our study. Instead, higher conductivity and concomitant acidity in high salinity stands of loblolly forest and across stands types in baldcypress forest could impose osmotic stress (ionic and acidic) on microbial communities, limiting microbial respiration regardless of C availability (Rath and Rousk, 2015). However, despite significantly greater conductivity and pH in baldcypress compared to loblolly forest, we found no difference in CO_2 fluxes between forest types, suggesting that biotic or abiotic factors other than pH and conductivity play a role in driving CO_2 fluxes across diverse coastal ecosystems.

In situ soil inundation, which can vary within forest types due to microtopography at the stand scale, can decrease the efficiency of microbial respiration to suppress CO_2 fluxes regardless of C supply or salinity (Megonigal et al., 2004). In loblolly forest, low salinity stands, which exist in slight depressions in the landscape, were fully saturated while high salinity stands were not. However, in baldcypress forest, soils were fully saturated across stand types. Driven by redox conditions, more efficient aerobic respiration in low mortality loblolly stands may produce more CO_2 relative to anaerobic respiration in saturated soils from high mortality loblolly stands and across stand types in baldcypress forest. Therefore, we show the potential for chemical or physical properties of coastal systems, such as soil inundation, to mask the effects of salinization and associated tree mortality on CO_2 fluxes.

4.2. Effect of chronic and pulsed salinity on CH_4 fluxes

Despite the putative capacity for saltwater intrusion to increase sulfate concentrations and suppress methanogenesis (Poffenbarger et al., 2011), our results show the opposite outcome with soils exposed to chronic and pulsed salinity exhibiting a greater potential for CH_4 emissions. These results suggest that other factors such as organic matter availability, and soil redox conditions may mediate the effect of salinity on methanogenesis and methanotrophy at our study site (Al-Haj and Fulweiler, 2020; Ardón et al., 2018; Seyfferth et al., 2020; Zhuang et al., 2018). Strikingly, CH_4 fluxes increased in response to chronic and pulsed salinity in a loblolly forest. Furthermore, we observed no interaction between the two scales of salinization with pulsed salinity driving increased CH_4 fluxes across both high and low salinity stands. Soil redox

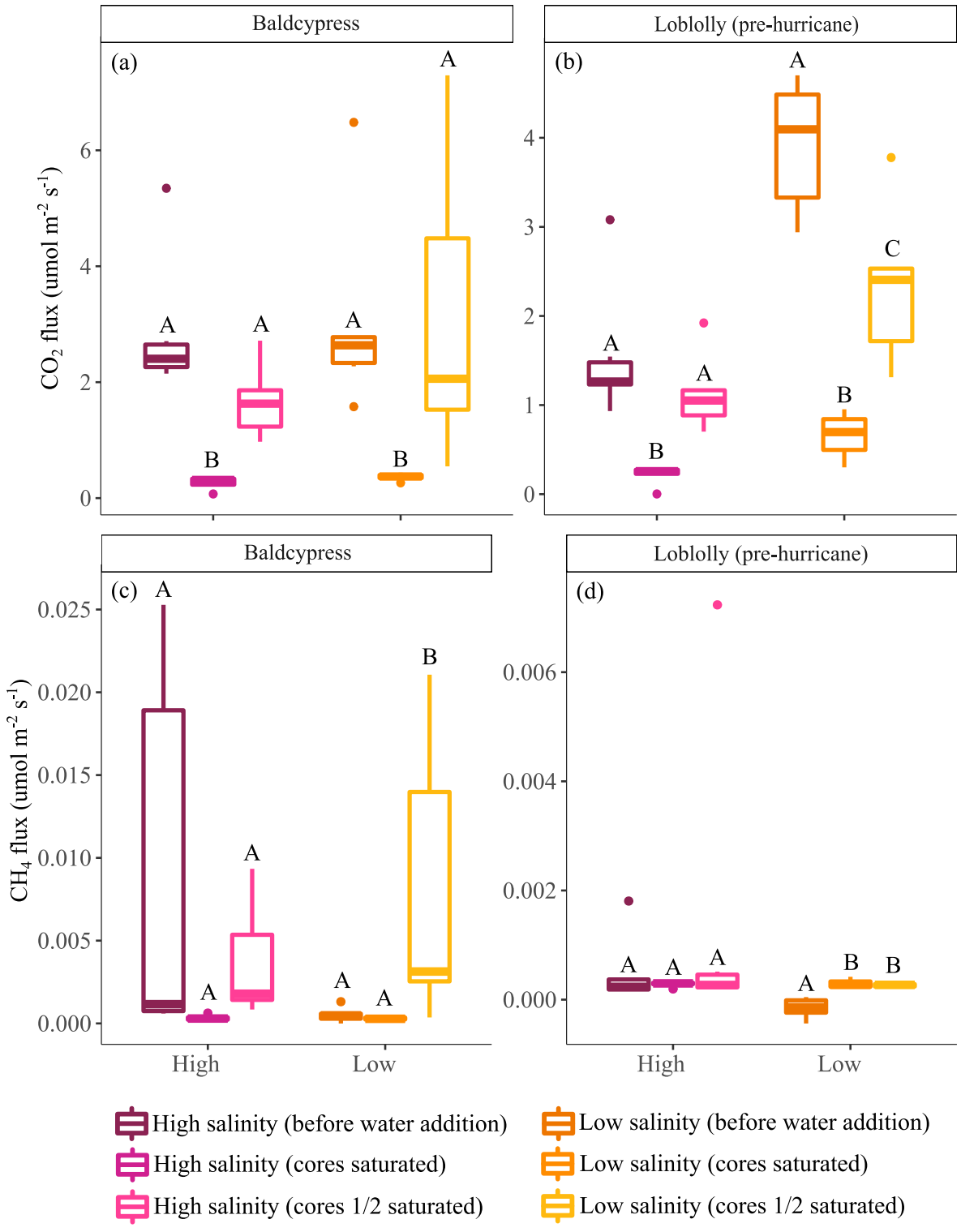

Fig. 5. Boxplots illustrating the effect of rainwater addition on carbon dioxide fluxes in soils from high and low salinity stands in (a) baldcypress forest and (b) pre-hurricane loblolly forest and on methane fluxes in soils from high and low salinity stands in (c) baldcypress forest and (d) pre-hurricane loblolly forest. Data from high and low salinity stands are represented by pink and orange, respectively with different shades of these colors representing the three water addition phases of our mesocosm experiment. Letters denote significant differences between the three water addition phases based on a Tukey post hoc analysis.

conditions could partially explain CH_4 flux patterns between stand types with saturated conditions promoting anaerobic methanogenesis in high salinity stands and aerated conditions promoting aerobic methanotrophy in low salinity stands. However, this mechanism does not explain increased CH_4 production in response to the hurricane related storm surge in high salinity loblolly stands which exhibited higher salinity and CH_4 fluxes, but similar soil moisture after, relative to before, Hurricane Ian. It is also possible that these results are influenced by sampling and transporting soil cores which may alter existing communities of methanogens and methane-oxidizing bacteria. However, we minimized this potential signal in our data by treating all samples identically, initiating gas flux measurements the same day as the samples were

collected, and by maintaining *in situ* soil structure using intact cores. Therefore, we provide four potential alternative mechanisms that could stimulate CH_4 emissions in response to salinization.

First, it is possible that abundant organic matter or use of noncompetitive substrate decreased competition between sulfate reducers and methanogens for substrate, allowing methanogenesis to proceed in the presence of more efficient sulfate reduction (King, 1984; Zhuang et al., 2018). Although sulfate reducers can outcompete methanogens for acetate and hydrogen (King, 1984), methylotrophic methanogens that utilize methylated organic matter as a substrate can co-occur with sulfate reducers when substrate for these processes is available (Yuan et al., 2019; Zhuang et al., 2018). Therefore, methylotrophic methanogenesis can be the dominant pathway for CH_4 production in sulfate-rich coastal soils (John Parkes et al., 2012; Zhuang et al., 2016), particularly where contributions of fresh organic matter are decomposed to contribute to methanol pools (Zhuang et al., 2014). As such, increased bioavailability of organic substrates in response to a storm surge (Wong et al., 2008) could increase substrate availability for methylotrophic methanogenesis, though this pathways does not always increase in response to saltwater addition (Dang et al., 2019). Second, salinization can increase soil ammonium concentrations through displacement of ammonium by salt cations on cation exchange sites and through decreased ammonium uptake by salt-stressed vegetation (Ardón et al., 2013; Jun et al., 2013; Weston et al., 2010; Widney et al., 2019). At our study site, soil and ground water ammonium concentrations have been shown to increase in response to a storm surge (Blood et al., 1991), potentially contributing to increased CH_4 production (Bodelier, 2011; Liu and Greaver, 2009). Third, greater CH_4 fluxes in higher salinity soils could be driven by decreased CH_4 consumption rather than increased CH_4 production because methanotrophs may be more sensitive to osmotic stress from heightened salinity compared to methanogens (Conrad et al., 1995; Segers, 1998). Finally, it is possible that chronic exposure to inundation and salinization in high salinity stands led to biotic adaptation and formation of a microbial community able to carry out methanogenesis in the presence of competition from sulfate reducers (Ardón et al., 2018; Hopple et al., 2022; Rocca et al., 2020). Overall, we provide important evidence that chronic saltwater intrusion due to sea level rise and pulsed salinity from storm surges have the potential to increase CH_4 fluxes from coastal forest soils. This finding indicates a need for future work that integrates detailed soil chemical and microbial community analyses to better understand the mechanistic drivers of CH_4 production in coastal forests subject to intensifying storm surges and sea level rise.

In our study, the effects of soil salinization from a storm surge were confounded with the effects of season; pre-hurricane soils were collected in May of 2022 and post-hurricane soils were collected in October of 2022. Production of labile C exudates, which can fuel CH_4 production (Waldo et al., 2019), and root oxygen loss, which can fuel CH_4 oxidation (King, 1994), may depend on root growth and therefore exhibit seasonality, potentially driving the observed increase in CH_4 fluxes after Hurricane Ian. However, CO_2 fluxes, which should also be affected by seasonal differences in labile C supply, were similar across sample dates. Furthermore, CH_4 emissions were greater in post-hurricane soils across stand types with this effect being greater in high salinity stands where most trees have died and labile C production would not be expected to exhibit seasonal patterns. Therefore, although our experimental design does not allow us to quantify the contribution of seasonality to observed greenhouse gas fluxes, we provide evidence that pulsed salinity from a storm surge may have played a role in stimulating CH_4 fluxes at our study site.

4.3. Effect of freshwater inundation on greenhouse gas fluxes

Intensifying rain events increase saturation of coastal forest soils, potentially mediating the effects of saltwater intrusion on greenhouse gas emissions particularly where microtopography can drive variation in soil saturation at a small spatial scale. Consistent with the theoretical expectation that soil saturation would cause a shift from aerobic to anaerobic microbial metabolism, we observed decreased CO_2 fluxes in fully saturated soils relative to field moist soils across stand types with different *in situ* soil salinity. However, CO_2 fluxes in half saturated soils were generally similar to CO_2 fluxes from field moist soils, such that suppressed CO_2 fluxes during full saturation may have been driven by slow diffusion of CO_2 through water (Troeh et al., 1982) rather than a switch to anaerobic respiration. Furthermore, we observed greater CH_4 production in half saturated relative to field moist soils in low salinity stands, but not high salinity stands across loblolly and baldcypress forests, suggesting that chronic salinization may mediate the transition to anaerobic respiration and methanogenesis when soils become saturated with rainwater. In loblolly forest, it is possible that differences in antecedent moisture conditions between high and low salinity stands explain this effect with rewetting of dry soils from low salinity stands causing a sudden increase in dissolved organic carbon available for microbial respiration, thus stimulating methanogenesis (Chow et al., 2006; Patel et al., 2021). However, there was no difference in *in situ* soil saturation between stand types in baldcypress forest suggesting that the greater effect of freshwater addition in soils from low salinity stands may be driven lower salinity rather than variation in *in situ* soil moisture. It is important to note that our lab incubations took place over one week with each phase lasting 24–72 hours and were therefore not long enough to document shifts in gas fluxes due to adaptation of microbial communities to altered soil moisture. However, our incubations were meant to simulate pulses of freshwater from intense tropical storms and therefore simulate processes that may change over this shorter time scale. Overall, our results suggest that salinization may suppress the effects of short-term rainwater inundation on CH_4 fluxes, highlighting the importance of studying the interactive effects of salinization and freshwater inundation in coastal systems that are increasingly exposed to both conditions.

4.4. Conclusions

Our study was uniquely designed to explore how localized abiotic conditions that cause tree mortality in coastal forests can affect greenhouse gas emissions, allowing us to investigate interactive effects of salinization, inundation and tree mortality and to assess the potential for stressed coastal systems to generate feedbacks with climate change. First, we found that patterns in CO_2 fluxes may have been primarily driven by *in situ* soil inundation, and secondarily by soil conductivity and pH, rather than by changes in SOM quantity or quality potentially caused by tree mortality, as we had originally hypothesized. Second, we showed that CH_4 fluxes can increase in response to pulsed salinity in a loblolly forest even though sulfate reducers are often thought to outcompete methanogens for substrate in higher salinity soils. We speculate that an influx of organic matter from the storm surge could have stimulated microbial respiration, with abundant substrate potentially decreasing competition between sulfate reducers and methanogens to drive greater CH_4 fluxes in higher salinity post-hurricane soils relative to lower salinity pre-hurricane soils. Finally, we showed that chronic salinization can decrease the effects of short-term rainwater inundation on CH_4 emissions, suggesting that soil salinity has the potential to affect the shift from aerobic to anaerobic respiration under partially inundated conditions. Future investigation of organic matter molecular composition and microbial community structure in dying coastal forests are needed to mechanistically understand the patterns in greenhouse gas emissions that we observed. However, we demonstrated that patterns in greenhouse gas emissions from stressed coastal systems can be context dependent and vary based on environmental covariates such as soil inundation, organic matter availability and pH. Furthermore, we highlight the importance of investigating interactive effects of salinization, inundation and tree mortality which often co-occur in stressed coastal systems and have the potential create feedbacks with climate change by altering soil greenhouse gas emissions.

Author contributions

GSS, TLO and ATC conceived of and designed the study; GSS, TLO and ATC designed and built the lab mesocosm; TLO and ATC acquired funding for the study. GSS conducted the field work, processed the samples, analyzed the results with help from TLO and wrote the manuscript; TLO and ATC edited the manuscript.

Declaration of competing interest

The authors declare the following financial interests/personal relationships which may be considered as potential competing interests: Georgia Seyfried reports financial support was provided by Clemson University. Thomas O'Halloran and Alex Chow reports financial support was provided by National Science Foundation.

Data availability

Data will be made available on request.

Acknowledgments

We appreciate field assistance from Kelly Cheah, Bo Song, Tom Williams, Michael Kline and Zane Ma. This material is based upon work supported by the National Science Foundation under Grants DBI-1828167 and DEB-1725377. GSS and this project were funded in part by Clemson University's RInitiative Program. Technical Contribution No. 7170 of the Clemson University Experiment Station.

Appendix A. Supplementary data

Supplementary data to this article can be found online at https://doi.org/10.1016/j.soilbio.2023.109101.

References

Al-Haj, A.N., Fulweiler, R.W., 2020. A synthesis of methane emissions from shallow vegetated coastal ecosystems. Global Change Biology 26, 2988–3005. https://doi.org/10.1111/gcb.15046.

Ardón, M., Helton, A.M., Bernhardt, E.S., 2018. Salinity effects on greenhouse gas emissions from wetland soils are contingent upon hydrologic setting: a microcosm experiment. Biogeochemistry 140, 217–232. https://doi.org/10.1007/s10533-018-0486-2.

Ardón, M., Morse, J.L., Colman, B.P., Bernhardt, E.S., 2013. Drought-induced saltwater incursion leads to increased wetland nitrogen export. Global Change Biology 19, 2976–2985. https://doi.org/10.1111/gcb.12287.

Armstrong, T., 2022. Hurricane Ian: September 230, 2022. National Weather Service [WWW Document].

Blood, E.R., Anderson, P., Smith, P.A., Nybro, C., Ginsberg, K.A., 1991. Effects of hurricane hugo on coastal soil solution chemistry in South Carolina. Biotropica 23, 348–355. https://doi.org/10.2307/2388251.

Bodelier, P.L.E., 2011. Interactions between nitrogenous fertilizers and methane cycling in wetland and upland soils. Current Opinion in Environmental Sustainability 3, 379–388. https://doi.org/10.1016/j.cosust.2011.06.002.

Capooci, M., Barba, J., Seyfferth, A.L., Vargas, R., 2019. Experimental influence of storm-surge salinity on soil greenhouse gas emissions from a tidal salt marsh. Science of the Total Environment 686, 1164–1172. https://doi.org/10.1016/j.scitotenv.2019.06.032.

Chambers, L.G., Reddy, K.R., Osborne, T.Z., 2011. Short-term response of carbon cycling to salinity pulses in a freshwater wetland. Soil Science Society of America Journal 75, 2000–2007. https://doi.org/10.2136/sssaj2011.0026.

Chen, H., Rücker, A.M., Liu, Y., Miller, D., Dai, J.-N., Wang, J.-J., Suhre, D.O., Kuo, L.-J., Conner, W.H., Campbell, B.J., Rhew, R.C., Chow, A.T., 2023. Unique biogeochemical characteristics in coastal ghost forests – the transition from freshwater forested wetland to salt marsh under the influences of sea level rise. Soil & Environmental Health 1, 100005. https://doi.org/10.1016/j.seh.2023.100005.

Chow, A.T., Tanji, K.K., Gao, S., Dahlgren, R.A., 2006. Temperature, water content and wet–dry cycle effects on DOC production and carbon mineralization in agricultural peat soils. Soil Biology and Biochemistry 38, 477–488. https://doi.org/10.1016/j.soilbio.2005.06.005.

Collin, M., Rasmuson, A., 1988. A comparison of gas diffusivity models for unsaturated porous Media. Soil Science Society of America Journal 52, 1559–1565. https://doi.org/10.2136/sssaj1988.03615995005200060007x.

Conrad, R., Frenzel, P., Cohen, Y., 1995. Methane emission from hypersaline microbial mats: lack of aerobic methane oxidation activity. FEMS Microbiology Ecology 16, 297–305. https://doi.org/10.1111/j.1574-6941.1995.tb00294.x.

Courtois, E.A., Stahl, C., Burban, B., den Berge, J., Berveiller, D., Bréchet, L., Soong, J.L., Arriga, N., Peñuelas, J., Janssens, I.A., 2019. Automatic high-frequency measurements of full soil greenhouse gas fluxes in a tropical forest. Biogeosciences 16, 785–796. https://doi.org/10.5194/bg-16-785-2019.

Dang, C., Morrissey, E.M., Neubauer, S.C., Franklin, R.B., 2019. Novel microbial community composition and carbon biogeochemistry emerge over time following saltwater intrusion in wetlands. Global Change Biology 25, 549–561. https://doi.org/10.1111/gcb.14486.

Dou, F., Ping, C.-L., Guo, L., Jorgenson, T., 2008. Estimating the impact of seawater on the production of soil water-extractable organic carbon during coastal Erosion. Journal of Environmental Quality 37, 2368–2374. https://doi.org/10.2134/jeq2007.0403.

Edmonds, J.W., Weston, N.B., Joye, S.B., Mou, X., Moran, M.A., 2009. Microbial community response to seawater amendment in low-salinity tidal sediments. Microbial Ecology 58, 558–568. https://doi.org/10.1007/s00248-009-9556-2.

Fagherazzi, S., Anisfeld, S.C., Blum, L.K., Long, E.V., Feagin, R.A., Fernandes, A., Kearney, W.S., Williams, K., 2019. Sea level rise and the dynamics of the marsh-upland boundary. Frontiers in Environmental Science 7.

Fraterrigo, J.M., Ream, K., Knoepp, J.D., 2018. Tree mortality from insect infestation enhances carbon stabilization in southern appalachian forest soils. Journal of Geophysical Research: Biogeosciences 123, 2121–2134. https://doi.org/10.1029/2018JG004431.

Gessler, A., Cailleret, M., Joseph, J., Schönbeck, L., Schaub, M., Lehmann, M., Treydte, K., Rigling, A., Timofeeva, G., Saurer, M., 2018. Drought induced tree mortality – a tree-ring isotope based conceptual model to assess mechanisms and predispositions. New Phytologist 219, 485–490. https://doi.org/10.1111/nph.15154.

Helton, A.M., Ardón, M., Bernhardt, E.S., 2019. Hydrologic context alters greenhouse gas feedbacks of coastal wetland salinization. Ecosystems 22, 1108–1125. https://doi.org/10.1007/s10021-018-0325-2.

Herbert, E.R., Schubauer-Berigan, J., Craft, C.B., 2018a. Differential effects of chronic and acute simulated seawater intrusion on tidal freshwater marsh carbon cycling. Biogeochemistry 138, 137–154. https://doi.org/10.1007/s10533-018-0436-z.

Herbert, E.R., Schubauer-Berigan, J., Craft, C.B., 2018b. Differential effects of chronic and acute simulated seawater intrusion on tidal freshwater marsh carbon cycling. Biogeochemistry 138, 137–154. https://doi.org/10.1007/s10533-018-0436-z.

Hopple, A.M., Pennington, S.C., Megonigal, J.P., Bailey, V., Bond-Lamberty, B., 2022. Disturbance legacies regulate coastal forest soil stability to changing salinity and inundation: a soil transplant experiment. Soil Biology and Biochemistry 169, 108675. https://doi.org/10.1016/j.soilbio.2022.108675.

Jackson, C.R., Vallaire, S.C., 2009. Effects of salinity and nutrients on microbial assemblages in Louisiana wetland sediments. Wetlands 29, 277–287. https://doi.org/10.1672/08-86.1.

John Parkes, R., Brock, F., Banning, N., Hornibrook, E.R.C., Roussel, E.G., Weightman, A. J., Fry, J.C., 2012. Changes in methanogenic substrate utilization and communities with depth in a salt-marsh, creek sediment in southern England. Estuarine. Coastal and Shelf Science 96, 170–178. https://doi.org/10.1016/j.ecss.2011.10.025.

Jun, M., Altor, A.E., Craft, C.B., 2013. Effects of increased salinity and inundation on inorganic nitrogen exchange and phosphorus sorption by tidal freshwater floodplain forest soils, Georgia (USA). Estuaries and Coasts 36, 508–518. https://doi.org/10.1007/s12237-012-9499-6.

Keiluweit, M., Wanzek, T., Kleber, M., Nico, P., Fendorf, S., 2017. Anaerobic microsites have an unaccounted role in soil carbon stabilization. Nature Communications 8, 1771. https://doi.org/10.1038/s41467-017-01406-6.

King, G.M., 1994. Associations of methanotrophs with the roots and rhizomes of aquatic vegetation. Applied and Environmental Microbiology 60, 3220–3227.

King, G.M., 1984. Utilization of hydrogen, acetate, and "noncompetitive"; substrates by methanogenic bacteria in marine sediments. Geomicrobiology Journal 3, 275–306.

King, J.Y., Reeburgh, W.S., Thieler, K.K., Kling, G.W., Loya, W.M., Johnson, L.C., Nadelhoffer, K.J., 2002. Pulse-labeling studies of carbon cycling in Arctic tundra ecosystems: the contribution of photosynthates to methane emission. Global Biogeochemical Cycles 16, 10–18. https://doi.org/10.1029/2001GB001456.

Kirwan, M.L., Gedan, K.B., 2019. Sea-level driven land conversion and the formation of ghost forests. Nature Climate Change 9, 450–457. https://doi.org/10.1038/s41558-019-0488-7.

Krauss, K.W., Duberstein, J.A., 2010. Sapflow and water use of freshwater wetland trees exposed to saltwater incursion in a tidally influenced South Carolina watershed. Canadian Journal of Forest Research 40, 525–535. https://doi.org/10.1139/X09-204.

Krauss, K.W., Duberstein, J.A., Doyle, T.W., Conner, W.H., Day, R.H., Inabinette, L.W., Whitbeck, J.L., 2009. Site condition, structure, and growth of baldcypress along tidal/non-tidal salinity gradients. Wetlands 29, 505–519. https://doi.org/10.1672/08-77.1.

Langston, A.K., Kaplan, D.A., Putz, F.E., 2017. A casualty of climate change? Loss of freshwater forest islands on Florida's Gulf Coast. Global Change Biology 23, 5383–5397. https://doi.org/10.1111/gcb.13805.

Liu, L., Greaver, T.L., 2009. A review of nitrogen enrichment effects on three biogenic GHGs: the CO2 sink may be largely offset by stimulated N2O and CH4 emission. Ecology Letters 12, 1103–1117. https://doi.org/10.1111/j.1461-0248.2009.01351.x.

Marton, J.M., Herbert, E.R., Craft, C.B., 2012. Effects of salinity on denitrification and greenhouse gas production from laboratory-incubated tidal forest soils. Wetlands 32, 347–357. https://doi.org/10.1007/s13157-012-0270-3.

McDowell, N.G., Ball, M., Bond-Lamberty, B., Kirwan, M.L., Krauss, K.W., Megonigal, J. P., Mencuccini, M., Ward, N.D., Weintraub, M.N., Bailey, V., 2022. Processes and mechanisms of coastal woody-plant mortality. Global Change Biology 28, 5881–5900. https://doi.org/10.1111/gcb.16297.

Megonigal, J.P., Hines, M.E., Visscher, P.T., 2004. Anaerobic metabolism: linkages to trace gases. Biogeochemistry.

Megonigal, P., Whalen, S., Tissue, D., Bovard, B., Albert, D., Allen, A., 1999. A plant-soil-atmosphere microcosm for tracing radiocarbon from photosynthesis through methanogenesis. Soil Science Society of America Journal 63. https://doi.org/10.2136/sssaj1999.03615995006300030033x.

Neubauer, S., 2013. Ecosystem responses of a tidal freshwater marsh experiencing saltwater intrusion and altered hydrology. Estuaries and Coasts 36, 491–507. https://doi.org/10.1007/s12237-01109455-x.

Neubauer, S.C., Megonigal, J.P., 2015. Moving beyond global warming potentials to quantify the climatic role of ecosystems. Ecosystems 18, 1000–1013. https://doi.org/10.1007/s10021-015-9879-4.

Norwood, M.J., Ward, N.D., McDowell, N.G., Myers-Pigg, A.N., Bond-Lamberty, B., Indivero, J., Pennington, S., Wang, W., Kirwan, M., Hopple, A.M., Megonigal, J.P., 2021. Coastal forest seawater exposure increases stem methane concentration. Journal of Geophysical Research: Biogeosciences 126, e2020JG005915. https://doi.org/10.1029/2020JG005915.

Olsson, L., Ye, S., Yu, X., Wei, M., Krauss, K.W., Brix, H., 2015. Factors influencing CO$_{2}$ and CH$_{4}$ emissions from coastal wetlands in the Liaohe Delta, Northeast China. Biogeosciences 12, 4965–4977. https://doi.org/10.5194/bg-12-4965-2015.

Patel, K.F., Myers-Pigg, A., Bond-Lamberty, B., Fansler, S.J., Norris, C.G., McKever, S.A., Zheng, J., Rod, K.A., Bailey, V.L., 2021. Soil carbon dynamics during drying vs. rewetting: importance of antecedent moisture conditions. Soil Biology and Biochemistry 156, 108165. https://doi.org/10.1016/j.soilbio.2021.108165.

Petrakis, S., Barba, J., Bond-Lamberty, B., Vargas, R., 2018. Using greenhouse gas fluxes to define soil functional types. Plant and Soil 423, 285–294. https://doi.org/10.1007/s11104-017-3506-4.

Petrakis, S., Seyfferth, A., Kan, J., Inamdar, S., Vargas, R., 2017. Influence of experimental extreme water pulses on greenhouse gas emissions from soils. Biogeochemistry 133, 147–164. https://doi.org/10.1007/s10533-017-0320-2.

Poffenbarger, H.J., Needelman, B.A., Megonigal, J.P., 2011. Salinity influence on methane emissions from tidal Marshes. Wetlands 31, 831–842. https://doi.org/10.1007/s13157-011-0197-0.

R Development Core Team, 2019. R: A Language and Environment for Statistical Computing. R Fouondataion for Statistical Computing, Vienna, Austria.

Rath, K.M., Rousk, J., 2015. Salt effects on the soil microbial decomposer community and their role in organic carbon cycling: a review. Soil Biology and Biochemistry 81, 108–123. https://doi.org/10.1016/j.soilbio.2014.11.001.

Rocca, J.D., Simonin, M., Bernhardt, E.S., Washburne, A.D., Wright, J.P., 2020. Rare microbial taxa emerge when communities collide: freshwater and marine microbiome responses to experimental mixing. Ecology 101, e02956. https://doi.org/10.1002/ecy.2956.

Russell, V.L., 2021. Emmeans: Estimated Marginal Means, Aka Least-Squares Means.

Segers, R., 1998. Methane production and methane consumption: a review of processes underlying wetland methane fluxes. Biogeochemistry 41, 23–51.

Sengupta, A., Stegen, J.C., Bond-Lamberty, B., Rivas-Ubach, A., Zheng, J., Handakumbura, P.P., Norris, C., Peterson, M.J., Yabusaki, S.B., Bailey, V.L., Ward, N. D., 2021. Antecedent conditions determine the biogeochemical response of coastal soils to seawater exposure. Soil Biology and Biochemistry 153, 108104. https://doi.org/10.1016/j.soilbio.2020.108104.

Servais, S., Kominoski, J.S., Charles, S.P., Gaiser, E.E., Mazzei, V., Troxler, T.G., Wilson, B.J., 2019. Saltwater intrusion and soil carbon loss: testing effects of salinity and phosphorus loading on microbial functions in experimental freshwater wetlands. Geoderma 337, 1291–1300. https://doi.org/10.1016/j.geoderma.2018.11.013.

Seyfferth, A.L., Bothfeld, F., Vargas, R., Stuckey, J.W., Wang, J., Kearns, K., Michael, H. A., Guimond, J., Yu, X., Sparks, D.L., 2020. Spatial and temporal heterogeneity of geochemical controls on carbon cycling in a tidal salt marsh. Geochimica et Cosmochimica Acta 282, 1–18. https://doi.org/10.1016/j.gca.2020.05.013.

Song, B., Gresham, C.A., Trettin, C.C., Williams, T.M., 2012. Recovery of coastal plain forests from Hurricane Hugo in South Carolina, USA, fourteen years after the storm. Tree and Forestry Science and Biotechnology 6, 60–68.

Spalding, E.A., Hester, M.W., 2007. Interactive effects of hydrology and salinity on oligohaline plant species productivity: implications of relative sea-level rise. Estuaries and Coasts 30, 214–225. https://doi.org/10.1007/BF02700165.

Stagg, C.L., Schoolmaster, D.R., Krauss, K.W., Cormier, N., Conner, W.H., 2017. Causal mechanisms of soil organic matter decomposition: deconstructing salinity and flooding impacts in coastal wetlands. Ecology 98, 2003–2018. https://doi.org/10.1002/ecy.1890.

Stuckey, B.N., 1982. Soil Survey of Georgetown. South Carolina, Georgetown, SC.

Troeh, F.R., Jabro, J.D., Kirkham, D., 1982. Gaseous diffusion equations for porous materials. Geoderma 27, 239–253.

Ulus, Y., Tsui, M.T.-K., Sakar, A., Nyarko, P., Aitmbarek, N.B., Ardón, M., Chow, A.T., 2022. Declines of methylmercury along a salinity gradient in a low-lying coastal wetland ecosystem at South Carolina, USA. Chemosphere 308, 136310. https://doi.org/10.1016/j.chemosphere.2022.136310.

Ury, E.A., Wright, J.P., Ardón, M., Bernhardt, E.S., 2022. Saltwater intrusion in context: soil factors regulate impacts of salinity on soil carbon cycling. Biogeochemistry 157, 215–226. https://doi.org/10.1007/s10533-021-00869-6.

Waldo, N.B., Hunt, B.K., Fadely, E.C., Moran, J.J., Neumann, R.B., 2019. Plant root exudates increase methane emissions through direct and indirect pathways. Biogeochemistry 145, 213–234. https://doi.org/10.1007/s10533-019-00600-6.

Wang, W., McDowell, N.G., Ward, N.D., Indivero, J., Gunn, C., Bailey, V.L., 2019. Constrained tree growth and gas exchange of seawater-exposed forests in the Pacific Northwest, USA. Journal of Ecology 107, 2541–2552. https://doi.org/10.1111/1365-2745.13225.

Weston, N.B., Dixon, R.E., Joye, S.B., 2006. Ramifications of increased salinity in tidal freshwater sediments: geochemistry and microbial pathways of organic matter mineralization. Journal of Geophysical Research: Biogeosciences 111. https://doi.org/10.1029/2005JG000071.

Weston, N.B., Giblin, A.E., Banta, G.T., Hopkinson, C.S., Tucker, J., 2010. The effects of varying salinity on ammonium exchange in Estuarine sediments of the parker river, Massachusetts. Estuaries and Coasts 33, 985–1003. https://doi.org/10.1007/s12237-010-9282-5.

Weston, N.B., Vile, M.A., Neubauer, S.C., Velinsky, D.J., 2011. Accelerated microbial organic matter mineralization following salt-water intrusion into tidal freshwater marsh soils. Biogeochemistry 102, 135–151. https://doi.org/10.1007/s10533-010-9427-4.

Widney, S.E., Smith, D., Herbert, E.R., Schubauer-Berigan, J.P., Li, F., Pennings, S.C., Craft, C.B., 2019. Chronic but not acute saltwater intrusion leads to large release of inorganic N in a tidal freshwater marsh. Science of the Total Environment 695, 133779. https://doi.org/10.1016/j.scitotenv.2019.133779.

Williams, T.M., Song, B., Trettin, C.C., Gresham, C.A., 2013. A review of spatial aspects of forest damage and recovery on the South Carolina coast following hurricane Hugo. Journal of Geography & Natural Disasters 3.

Wong, V.N.L., Dalal, R.C., Greene, R.S.B., 2008. Salinity and sodicity effects on respiration and microbial biomass of soil. Biology and Fertility of Soils 44, 943–953. https://doi.org/10.1007/s00374-008-0279-1.

Xiong, Y., D'Atri, J.J., Fu, S., Xia, H., Seastedt, T.R., 2011. Rapid soil organic matter loss from forest dieback in a subalpine coniferous ecosystem. Soil Biology and Biochemistry 43, 2450–2456. https://doi.org/10.1016/j.soilbio.2011.08.013.

Xu, C., Wong, V.N.L., Reef, R.E., 2021. Effect of inundation on greenhouse gas emissions from temperate coastal wetland soils with different vegetation types in southern Australia. Science of the Total Environment 763, 142949. https://doi.org/10.1016/j.scitotenv.2020.142949.

Yuan, J., Liu, D., Ji, Y., Xiang, J., Lin, Y., Wu, M., Ding, W., 2019. Spartina alterniflora invasion drastically increases methane production potential by shifting methanogenesis from hydrogenotrophic to methylotrophic pathway in a coastal marsh. Journal of Ecology 107, 2436–2450. https://doi.org/10.1111/1365-2745.13164.

Zhuang, G.-C., Elling, F.J., Nigro, L.M., Samarkin, V., Joye, S.B., Teske, A., Hinrichs, K.-U., 2016. Multiple evidence for methylotrophic methanogenesis as the dominant methanogenic pathway in hypersaline sediments from the Orca Basin, Gulf of Mexico. Geochimica et Cosmochimica Acta 187, 1–20. https://doi.org/10.1016/j.gca.2016.05.005.

Zhuang, G.-C., Heuer, V.B., Lazar, C.S., Goldhammer, T., Wendt, J., Samarkin, V.A., Elvert, M., Teske, A.P., Joye, S.B., Hinrichs, K.-U., 2018. Relative importance of methylotrophic methanogenesis in sediments of the Western Mediterranean Sea. Geochimica et Cosmochimica Acta 224, 171–186. https://doi.org/10.1016/j.gca.2017.12.024.

Zhuang, G.-C., Lin, Y.-S., Elvert, M., Heuer, V.B., Hinrichs, K.-U., 2014. Gas chromatographic analysis of methanol and ethanol in marine sediment pore waters: validation and implementation of three pretreatment techniques. Marine Chemistry 160, 82–90. https://doi.org/10.1016/j.marchem.2014.01.011.